Available online at www.sciencedirect.com
SCIENCE DIRECT®
Journal of Organometallic Chemistry 689 (2004) 1978–1990
Journal of Organometallic Chemistry
www.elsevier.com/locate/jorganchem

# Comparative reactivity studies of dppf-containing $CpRu^{II}$ and $(C_6Me_6)Ru^{II}$ complexes towards different donor ligands (dppf = 1,1′-bis(diphenylphosphino)ferrocene)

Xiu Lian Lu, Jagadese J. Vittal, Edward R.T. Tiekink, G.K. Tan, Seah Ling Kuan, Lai Yoong Goh *, T.S. Andy Hor *

*Department of Chemistry, National University of Singapore, Kent Ridge, Singapore 117543, Singapore*

Received 27 January 2004; accepted 18 March 2004

**Abstract**

[CpRu(dppf)Cl] (Cp = $\eta^5$-$C_5H_5$) (**1**) and [(HMB)Ru(dppf)Cl]$PF_6$ ((HMB) = $\eta^6$-$C_6Me_6$) (**3**) react with different donor ligands to give rise to N-, P- and S-bonded complexes. The stoichiometric reactions of **1** and **3** with NaNCS give the mononuclear complexes [CpRu(dppf)(NCS)] (**2**) and [(HMB)Ru(dppf)(NCS)]$PF_6$ (**4**), respectively, in yields above 80%, while **3** also gives a dppf-bridged diruthenium complex [(HMB)Ru$(NCS)_2]_2$(μ-dppf) (**5**) in 67% yield from reaction with four molar equivalents of NaNCS. Compound **5** is also obtained in 70% yield from the reaction of **4** with excess NaNCS. With $CH_3CN$ in the presence of salts, both **1** and **3** give their analogous solvento derivatives [CpRu(dppf)$(CH_3CN)$]$BPh_4$ (**6**) and [(HMB)Ru(dppf)$(CH_3CN)$] $(PF_6)_2$ (**7**). With phosphines, the reaction of **1** gives chloro-displaced complexes [(CpRu(dppf)L]$PF_6$ (L = $PMe_3$ (**8**), $PMe_2Ph$(**9**)), whereas the reaction of **3** with $PMe_2Ph$ leads to substitution of dppf, giving [(HMB)Ru$(PMe_2Ph)_2$Cl] $PF_6$ (**10**). The reaction of **1** with $NaS_2CNEt_2$ gives a dinuclear dppf-bridged complex [{CpRu$(S_2CNEt_2)$}$_2$(μ-dppf)] (**11**), whereas that of **3** results in loss of the HMB ligand giving a mononuclear complex [Ru(dppf)$(S_2CNEt_2)_2$] (**12**). With elemental sulfur $S_8$, **1** is oxidized to give a dinuclear $CpRu^{III}$ dppf-chelated complex [{CpRu(dppf)}$_2$(μ-$S_2$)]$(BPh_4)$Cl (**13**), whereas **3** undergoes oxidation at the ligand, giving a dppf-displaced complex [(HMB)Ru$(CH_3CN)_2$Cl]$PF_6$ (**14**) and free dppf$S_2$. The structures of **1**, **2**, **5**–**9**, **11**, **13** and **14** were established by X-ray single crystal diffraction analyses. Of these, **5** and **11** both contain a dppf-bridge between $Ru^{II}$ centers, while **13** is a dinuclear $CpRu^{III}$ disulfide-bridged complex; all the others are mononuclear. All complexes obtained were also spectroscopically characterized.


*Keywords:* Ruthenium; 1,1′-bis(diphenylphosphino)ferrocene; Cyclopentadienyl; Hexamethylbenzene; Disulfide; Crystal structures

## 1. Introduction

The organometallic chemistry of [CpRu$(PR_3)_2$Cl] [1,2] has been extensively studied and the related $\eta^6$-arene complexes are also known [3]. However, little is reported of their comparative reactivities. The electronic and steric differences of these aromatic π-ligands could confer on a metal complex different chemical and catalytic reactivity features [4,5]. Such differences could be exemplified when the potentially bidentate 1,1′-bis(diphenylphosphino)ferrocene (dppf) is used as the phosphine ligand. This ligand has attracted our recent interest because of its coordination variability and the catalytic potential it can confer on a complex [6,7]. $d^6$-$Ru^{II}$ complexes containing dppf are known [7] with about 20 crystallographic reports. These include three-legged piano-stool structures [$(C_5R_5)$Ru(dppf)H] (R = Me [8]; R = H [9]), [($\eta^6$-arene)Ru(dppf)Cl]$PF_6$ (arene = HMB [10], *p*-cymene [11]), [($\eta^6$-$Me_4$-$C_6H_2$)$RuCl_2]_2$(μ-dppf) · $CH_2Cl_2$ [10], [CpRu(dppf)(C≡C-($C_5H_4$NH))-$W(CO)_4(PPh_3)$] [12], [TpRu(dppf)Cl] and [Tp(dppf) Ru=C=C=$CPh_2$]$SbF_6$ [13] (Tp = tris(pyrazolyl)borate), a four-legged piano-stool complex [Cp*Ru(dppf)($\eta^2$-$O_2$)]$BF_4$ [14], and other octahedral structures [Ru-(dppf)$(bipy)_2$]$(PF_6)_2$ [15], [Ru(dppf)(CO)$(PPh_3)$(Cl)H] [16], [Ru(dppf)(CO)(NCMe)$(PPh_3)$H]$BF_4$ · EtOH [17],

* Corresponding authors. Tel.: +65-68742677; fax: +65-67791691.
*E-mail addresses:* chmgohly@nus.edu.sg (L.Y. Goh), andyhor@nus.edu.sg (T.S.A. Hor).

0022-328X/$ - see front matter © 2004 Elsevier B.V. All rights reserved.
doi:10.1016/j.jorganchem.2004.03.022

$[Ru(dppf)(C_3H_5)(C_6F_5O_2)]$ [18], $[RuCl(CO)(dppf)(PPh_3)]BF_4$ and $[RuCl(CO)(dppf)(CH_3CN)]_2(BF_4)_2$ [19]. In this paper we report complexes obtained by chloro substitution in [CpRu(dppf)Cl] (**1**) and [(HMB)Ru(dppf)Cl]$(PF_6)$ (**3**), and structural variations in response to the aromatic ring ligand.

## 2. Results and discussion

### 2.1. Synthesis

#### 2.1.1. Preparation of [CpRu(dppf)Cl] (1)

[CpRu(dppf)Cl] (**1**) was obtained as bright yellow solids in 78% yield from the reaction of $[CpRu(PPh_3)_2Cl]$ with dppf in refluxing toluene, according to the method of Bruce et al. [9].

#### 2.1.2. Reactions with N-donor ligands

*2.1.2.1. With NaNCS.* At ambient temperature, [CpRu(dppf)Cl] (**1**) reacted with one molar equivalent of NaNCS in MeOH, giving a yellow precipitate of [CpRu(dppf)(NCS)] (**2**) in 80% yield. Similar ligand replacement occurred with $[(HMB)Ru(dppf)Cl]PF_6$ (**3**) in refluxing MeOH for 23 h to give $[(HMB)Ru(dppf)(NCS)]PF_6$ (**4**) in 88% yield (shown in Scheme 1). With four molar equivalents of NaNCS, **3** gave rise to the diruthenium compound $[(HMB)Ru(NCS)_2]_2$(μ-dppf) (**5**) in 67% yield. The loss of chelating dppf can be diagnosed by NMR ($^1H$ and $^{31}P\{^1H\}$). Complex **5** can be independently synthesized (70% yield) from **4** with a stoichiometric excess of NaNCS. In contrast, **2** is inert towards excess NaNCS; this is possibly due to the greater electron-donating capability of the Cp ligand which results in stronger Ru–P bonds, thus preventing partial cleavage required for the conversion of $\eta^2$-dppf to μ-dppf in the dinuclear complex. The coordination site vacated by the chelate opening is taken up by the incoming thiocyanate. Although the latter can also function as a bridging ligand, it stays terminal and N-bonded in this case, thus allowing the dppf to switch its function to a bridging mode. Complex **5** therefore has the same structural type (see below) as the bridged complex $[(arene)RuCl_2]_2$(-dppf), which was obtained directly from a dinuclear precursor, $[(arene)RuCl_2]_2$ (arene = *p*-cymene, HMB, 1,2,3,4-$Me_4C_6H_2$, 1,2,3,5-$Me_4C_6H_2$) through dppf addition (Scheme 2) [10].

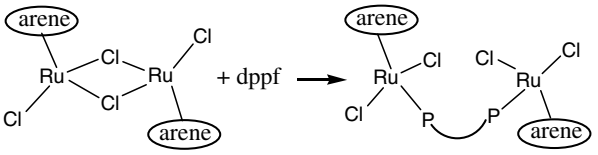


Scheme 2.

*2.1.2.2. With $CH_3CN$.* It is well established that the chloro ligands in Cp- or arene-ruthenium complexes can be abstracted by silver salts, giving solvento derivatives which can be isolated or allowed to react in situ with selected substrates [20]. We noted that [Cp*Ru(dppf)Cl] (Cp* = $\eta^5$-$C_5Me_5$) in $CH_3CN$ in the presence of $AgBF_4$ gave the solvento complex $[Cp^*Ru(dppf)(CH_3CN)]BF_4$, which could be used as a precursor to substitution products [14]. Here, we are interested in the acetonitrile derivatives of **1** and **3** to allow a comparison of their chemical reactivities. It was found that the chloro ligand in **1** was easily abstracted with $NaBPh_4$ in $CH_3CN$ within 1 h at room temperature to give $[CpRu(dppf)(CH_3CN)]BPh_4$ (**6**) in 80% yield; the analogous reaction of **3** with $NH_4PF_6$ in $CH_3CN$ had to be performed at reflux for 24 h, giving $[(HMB)Ru(dppf)(CH_3CN)](PF_6)_2$ (**7**) in 62% yield (Scheme 3). This reactivity difference probably arises from a greater resistance to remove an

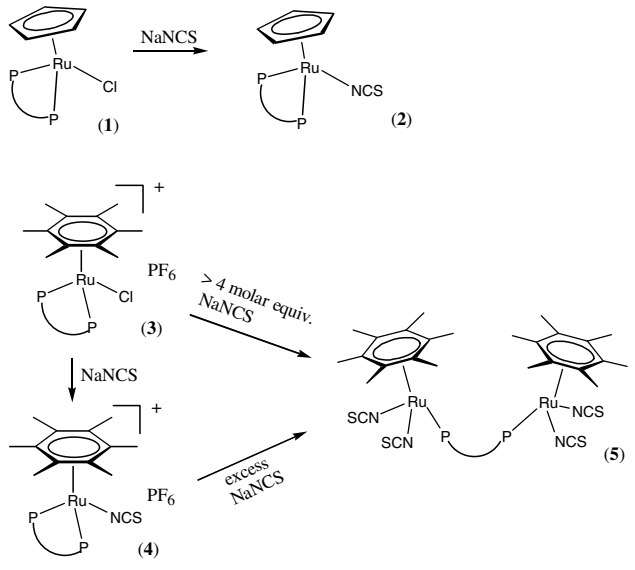


Scheme 1.

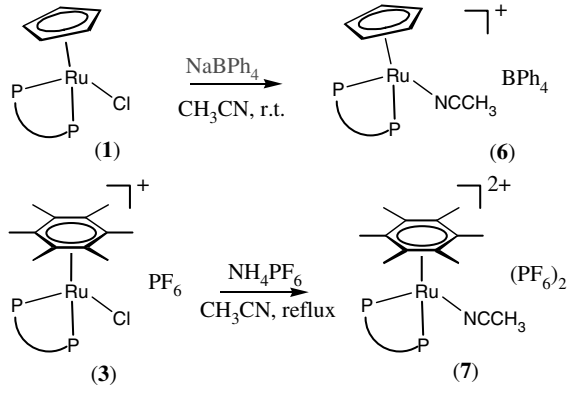


Scheme 3.

anionic ligand ($Cl^-$) from a monocationic core in **3**, as compared to a neutral core in **1**.

*2.1.3. Reactions with monophosphines*

Complex **1** undergoes chloro-substitution with the phosphines $PMe_3$ and $PMe_2Ph$ to give high yields of the expected monomeric cationic complexes $[CpRu(dppf)(PMe_3)]^+$ (**8**) and $[CpRu(dppf)(PMe_2Ph)]^+$ (**9**), isolated as their $PF_6^-$ salts after metathesis with $NH_4PF_6$ (Scheme 4). In contrast, the same reaction of $[(HMB)Ru(dppf)Cl]PF_6$ (**3**) with one or two molar equivalents of $PMe_2Ph$ in $CH_3CN$, resulted in displacement of dppf to give the complex $[(HMB)Ru(PMe_2Ph)_2Cl]PF_6$ (**10**) and free dppf (Scheme 5).

*2.1.4. With S-donor ligands*

*2.1.4.1. With $NaS_2CNEt_2$.* The reaction of **1** with slightly more than one molar equivalent of sodium diethyl dithiocarbamate, $NaS_2CNEt_2$, in MeOH under reflux gave a yellow dinuclear complex $[CpRu(S_2CNEt_2)_2]_2(\mu$-dppf) (**11**) (75% yield). Like the thiocyanate complex **5**, the formation of **11** involved halide loss and release of a free dppf ligand, with the concomitant change from chelating $\eta^2$- to a $\mu$-bonding mode for dppf (Scheme 6). In comparison, the analogous reaction of [CpRu(dppe)Cl] was reported to give the mononuclear complex $[CpRu(dppe)(S_2CNEt_2)]$ [21] (Scheme 6). The ability for dppf to take to bridging allows the dithiocarbamate to adopt its usual chelating mode.

A similar reaction of $[(HMB)Ru(dppf)Cl]PF_6$ (**3**) with $NaS_2CNEt_2$ led to a product mixture from which $[Ru(S_2CNEt_2)_2(dppf)]$ (**12**) was separated in 26% yield from free hexamethylbenzene ligand and other non-isolable unstable products. The formation of **12** resulted from loss of halide and an unexpected cleavage of the arene ligand in **3** (Scheme 7). The loss of arene ligand is electronically compensated by the introduction of two chelating dithiocarbamates into the coordination sphere. Similar loss of the Cp ligand on **1** was not expected due to the anionic nature of the Cp ligand. We have previously reported a direct synthesis of **12** from the reaction of $[Ru(S_2CNEt_2)_2(PPh_3)_2]$ with dppf ligand in 80% yield [22].

*2.1.4.2. With elemental sulfur*. The reactions of **1** and **3** with elemental sulfur have also been studied. An ambient temperature reaction of **1** with $S_8$ in the presence of $NaBPh_4$ gave deep-green solids of diruthenium$^{III}$ $[\{CpRu(dppf)\}_2(\mu_2\text{-}S_2)](BPh_4)Cl$ (**13**) in 69% yield (Scheme 8). The microanalytical data and X-ray diffraction analysis (see below) both show the presence of the "mixed" anions, which was not expected in the presence of excess $NaBPh_4$. Thus Ru(II) in **1** has been oxidized to Ru(III) giving the 34e disulfide species **13**. Rauchfuss and co-workers had prepared the bis($PPh_3$) analogue of **13** from the reaction of $CpRu(PPh_3)_2Cl$ with $S_8$ in the presence of $AgBF_4$ [23a] or the air-oxidation of $CpRu(PPh_3)_2SH$ and of $[CpRu(PPh_3)_2(H_2S)]^+$ [23b].

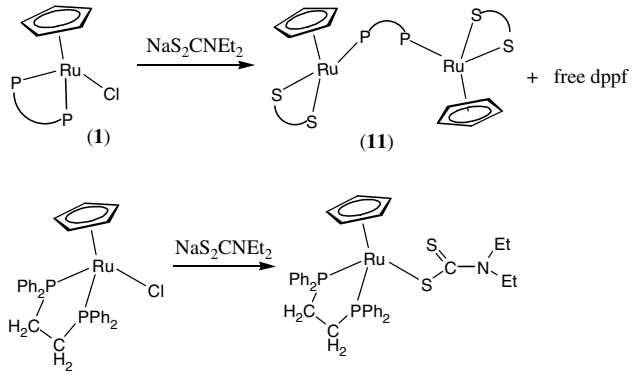


Scheme 6.

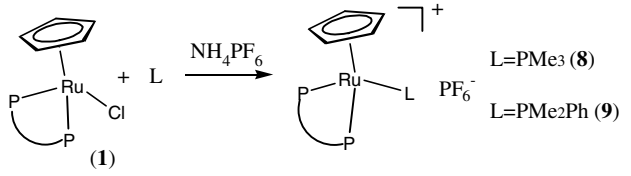


Scheme 4.

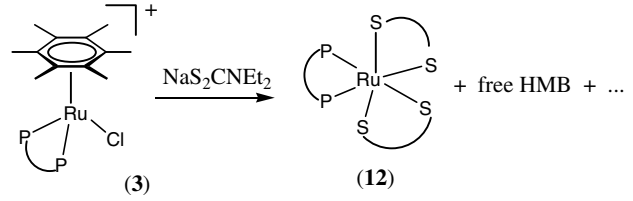


Scheme 7.

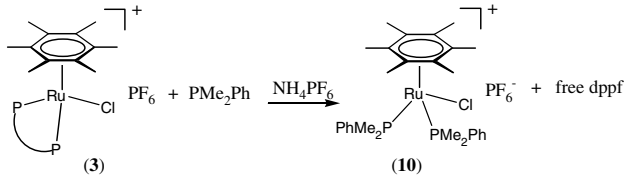


Scheme 5.

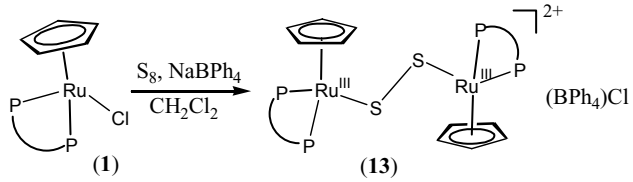


Scheme 8.

Instead of undergoing loss of halide ligand as in **1**, the arene complex [(HMB)Ru(dppf)Cl]$PF_6$ (**3**) reacted with loss of dppf in the presence of $NH_4PF_6$ in $CH_3CN$ to give [(HMB)Ru$(CH_3CN)_2$Cl]$PF_6$ (**14**) as an orange solid in 63% yield and free dppf($S_2$) (30% yield) [23] as a yellow-solid, which was identified via its elemental analysis together with its NMR and FAB-MS spectra (Scheme 9). Complex **14** could also be obtained from the reaction of [(HMB)$RuCl_2]_2$ with $NH_4PF_6$ in $CH_3CN$ in 90% yield [11]. The arene ligand appears to protect the metal from oxidation. Instead, the dppf ligand is oxidized and cleaved. Oxidative sulfurization of coordinated dppf with elemental sulfur has been observed in Pt$(dppf)_2$ at room temperature (Scheme 10) [24]. Conversion of free dppf to dppf($S_2$) usually requires thermal activation, e.g. in refluxing 1-butanol [25]. Such conversion however could be catalyzed by metal under ambient condition; for example, through the insertion of S into Ru–P bond, prior to departure of the labile dppf($S_2$) ligand.

### 2.2. Spectral characteristics

Details of the spectral features of the product complexes are given in Section 4. Only some significant comparisons are noted here. Except for the disulfur-bridged paramagnetic CpRu(III) complex **13**, all the CpRu(II) complexes show a sharp resonance for the $\eta^5$-$C_5H_5$ protons in the range $\delta$ 4.29–4.75, while the (arene)Ru(II)dppf complexes show the Me resonance of HMB as singlets at $\delta$ 1.51–1.77 in the proton NMR spectrum. The non-dppf (arene)Ru complexes **10** and **14** show proton signals for Me of HMB at $\delta$ 1.67 and 2.13, respectively. The $C_5H_4$ protons of the dppf ligands are observed in the range $\delta$ 3.96–4.96 as four equal-intensity peaks for the CpRu complexes **2** and **9** and for the (HMB)Ru complexes **4** and **7**, or as a pair of peaks of equal intensity for the CpRu complexes **6**, **8** and **11**. The corresponding resonance for the (μ-dppf)(HMB)Ru complex **5** appears as a broad unresolved multiplet, presumably due to fluxionality. The $^{31}P$ resonance of dppf of the CpRu(II) complexes are observed at $\delta$ 46.1–49.8, with those of complexes **8** and **9** appearing as doublets due to P–P coupling ($J = 42$ Hz) with the monophosphine co-ligand, viz. $PMe_3$ and $PMe_2Ph$, respectively. Correspondingly, the $PMe_3$ and $PMe_2Ph$ signals are seen as triplets due to coupling to the two P atoms of dppf. While the $^{31}P$ resonances of the dppf ligand in the (arene)Ru complexes **4** and **7** are observed within a narrow range ($\delta$ 38.4, 34.2), that of (μ-dppf) **5** is found in a much higher field ($\delta$ 27.3).

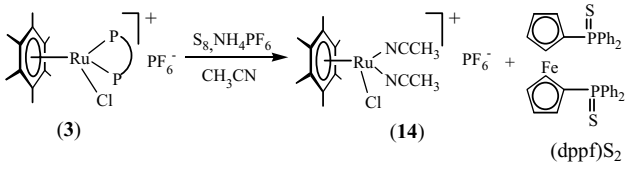


(**3**) (**14**) (dppf)$S_2$

Scheme 9.

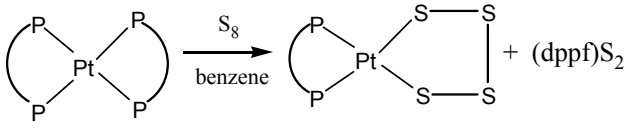


Scheme 10.

The $FAB^+$-mass spectra of the CpRu complexes and (HMB)Ru complexes **4**, **10** and **14** display the corresponding parent $M^+$ ions; however, the mother ions are not observed for the (μ-dppf) (arene)Ru complex **5** and the complex **7**, indicating that the bis($CH_3CN$) monocationic complex **14** is more stable than the mono-($CH_3CN$) dicationic complex **7** in the $FAB^+$ mass beam.

Infrared spectra (KBr) show strong bands due to $\nu_{C\equiv N}$ and $\nu_{C-S}$ of the NCS ligand: **2** (2105 and 697 $cm^{-1}$), **4** (2100 and 698 $cm^{-1}$) and **5** (2106 and 699 $cm^{-1}$). In comparison, it is noted that the $\nu_{C\equiv N}$ stretching frequencies in [CpRu$(SbPh_3)$(py)(NCS)] [26], $(Bu_4N)_2$[Ru$(dcpyH)_2(NCS)_2$] [27] and [Ru(NCS)(NO)-(bpy)$(py)_2$]$(PF_6)_2$ [28] were found at 2030, 2120 and 2097 $cm^{-1}$, respectively, with $\nu_{C-S}$ at 808, 780 $cm^{-1}$ and in the $\nu_{PF6}$ region, respectively. The $\nu_{C\equiv N}$ stretching vibration of coordinated acetonitrile is seen at 2259 $cm^{-1}$ in **6**, 2363 $cm^{-1}$ in **7** and 2359 $cm^{-1}$ in **14**. The dithiocarbamate complexes **11** and **12** show $\nu$(CN) at 1486/1485 $cm^{-1}$, $\nu(NC_2)$ at 1146/1144 $cm^{-1}$ and $\nu$(CS) at 792/695 $cm^{-1}$.

### 2.3. X-ray structural studies

#### 2.3.1. The mononuclear complexes

In all cases, selected geometric parameters are given in their respective figure captions.

Since the X-ray single-crystal structure of **1** has not been reported, an analysis is included here for comparison with chloro-substituted derivatives. The molecular structure is given in Fig. 1. It shows a mononuclear Ru(II) capped by an $\eta^5$-Cp ring, a chelating $\eta^2$-dppf and a terminal chloride, thus completing a three-legged piano-stool configuration. The Ru–Cl bond distance of 2.4446(12) Å and Ru–P distances of 2.2871(12) and 2.2852(12) Å in **1** are virtually indistinguishable from those found in the dppe analogue, [CpRu(dppe)Cl] [29,30] (2.4466(7), 2.2688(7) and 2.2863(7) Å, respectively) [30]. The larger bite size of dppf forces a wider P–Ru–P chelate angle (95.01(4)° in **1** compared with 83.48(2)° in [CpRu(dppe)Cl]. The conformation of the Cp rings of dppf is best described as *synperiplanar eclipsed* as reflected in the torsion angle defined by

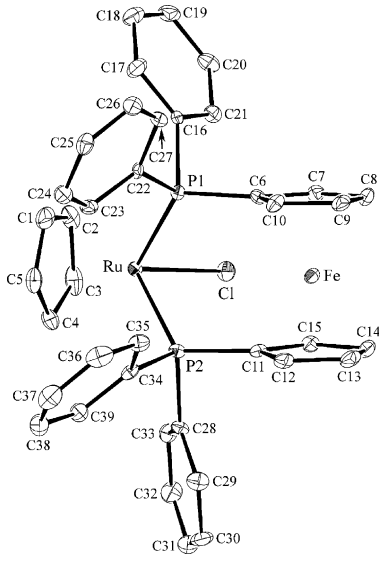


Fig. 1. Molecular structure of [CpRu(dppf)Cl] (**1**). Hydrogen atoms are omitted for clarity. Selected geometric parameters (Å, °): Ru–Cl 2.4446(12), Ru–P1 2.2871(12), Ru–P2 2.2852(12), Cl–Ru–P1 93.18(4), Cl–Ru–P2 89.47(4) and P1–Ru–P2 95.01(4).

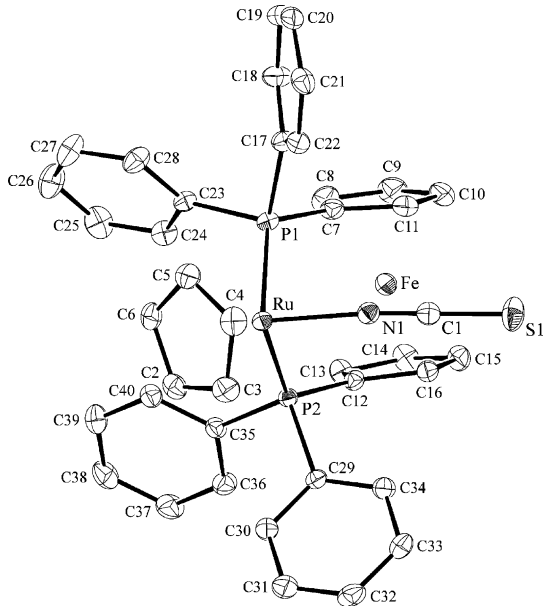


Fig. 2. Molecular structure of [CpRu(dppf)(NCS)] (**2**). Hydrogen atoms are omitted for clarity. Selected geometric parameters (Å, °): Ru–P1 2.2978(8), Ru–P2 2.2922(7), Ru–N1 2.076(3), P1–Ru–P2 96.77(3), P1–Ru–N1 88.91(7), P2–Ru–N1 87.22(7), Ru–N1–C1 173.1(2), N1–C1–S1 178.1(3).

P-ring centroids-P of 4.81(7)° [7]. The Cp rings are symmetrically disposed about the Fe atom so that both Fe-ring centroid distances are 1.648(2), the ring centroids subtend an angle of 178.26(12)° at Fe and the dihedral angle between the two Cp rings is 3.4(3)°.

The molecular structure of **2** is shown in Fig. 2. The compound co-crystallized with a solvent molecule of acetone so that the ratio of complex to acetone is 1:1. This mononuclear structure is similar to that of **1** with NCS replacing the chloride. The closest available structure for comparison is that of $[CpRu(PPh_3)_2(NCS)]$ [31] which also features an N-bound NCS ligand. The Ru–N bond distances are indistinguishable in the two structures but the Ru–P bond distances in **2** (2.2978(8) and 2.2922(7) Å) are significantly shorter than those in $[CpRu(PPh_3)_2(NCS)]$ (2.318(1) and 2.323(2) Å) [31]. The distance between the ring centroid of the Ru-bound Cp ring and the metal is 1.8596(14) Å. The conformation of the dppf-Cp rings is *synperiplanar eclipsed*; torsion angle 0.89(5)°, the Fe-ring centroid distances are 1.6414(16) and 1.6385(15) Å, the angle subtended at Fe is 176.43(8)° and the dihedral angle between the two Cp rings is 3.7(2)°.

The molecular structures of $[CpRu(dppf)(CH_3CN)]^+$ (**6**) and the dicationic HMB analogue **7** are similar and are given in Figs. 3(a) and (b). They possess a geometry at Ru similar to that adopted by **1** and **2** above, namely with capping Cp/HMB, $\eta^2$-dppf and N-coordinated $CH_3CN$ completing the three-legged piano-stool configuration. The C≡N bond length are 1.143(2) and 1.151(10) Å in **6** and **7**, respectively.

The molecular structure of the cation of **14** (Fig. 4) is included here to provide a comparison of some of its bond parameters with those of the chloro complex **1** and the $CH_3CN$ solvento complexes **6** and **7**. It is shown that a plane of symmetry through Ru and Cl bisects the HMB ring in **14**. The Ru–Cl bond (2.3975(8) Å) is shorter and presumably stronger than that in **1** (2.4446(12) Å). The Ru–N($CH_3CN$) distance (2.072(2) Å) is slightly longer than those in **6** and **7** (2.0487(16) and 2.018(7) Å, respectively). The C–N bond length of $CH_3CN$ is 1.1329(3), slightly shorter than those in **6** and **7**.

Likewise the molecular structures of the cations of **8** and **9**, shown in Fig. 5, belong to the monomeric type described above, with a similar geometry at the Ru center. The Ru–P distances (from 2.3436(11) and 2.3288(10) Å in **9** to 2.357(2) and 2.3244(18) Å in **8**) are shorter than those of the Cp*Ru(dppf) complex, e.g. 2.408(3) and 2.390(3) Å in $[Cp^*Ru(dppf)(\eta^2\text{-}O_2)]BF_4$ [14], but slightly longer than those of the ruthenium carboxylate phosphine complexes. The Ru–C distances between Cp and Ru metal increase in the order of **9** > **8** > **6**, indicating that the more bulky ligands have decreased the bond length.

### 2.3.2. The dinuclear complexes

As for the mononuclear complexes, selected geometric parameters are given in the figure captions.

The molecular structure of **5** is shown in Fig. 6. The molecule has crystallographic 2-fold symmetry such that the Fe atom lies on this axis and the structure co-crystallizes with a solvent water molecule that also lies on a

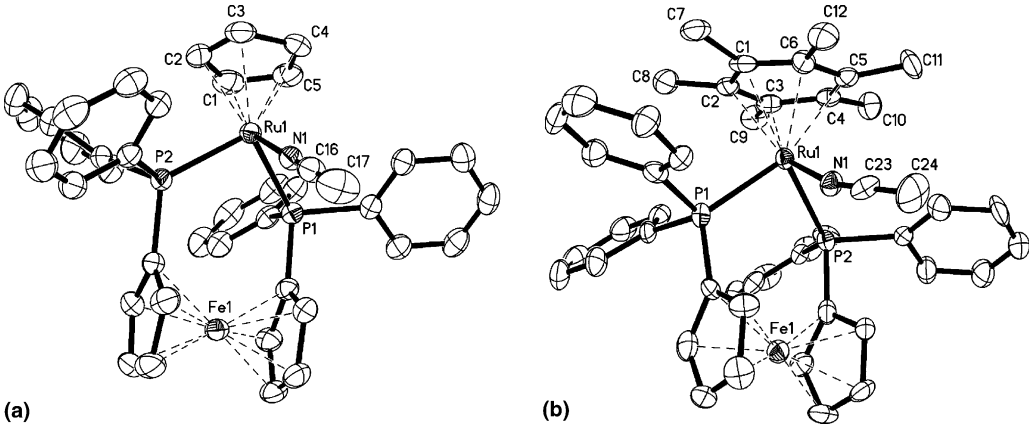


Fig. 3. (a) Molecular structure of $[CpRu(dppf)(CH_3CN)]^+$ (**6** cation). Hydrogen atoms are omitted for clarity. Selected geometric parameters (Å, °): Ru1–P1 2.3243(5), Ru1–P2 2.3206(5), Ru1–N1 2.0487(16), P1–Ru1–P2 98.702(18), P1–Ru1–N1 91.04(4), P2–Ru1–N1 87.89(4). (b) Molecular structure of $[(HMB)Ru(dppf)(CH_3CN)]^{2+}$ (**7** cation). Hydrogen atoms are omitted for clarity except in $CH_3CN$. Selected geometric parameters (Å, °): Ru1–P1 2.368(2), Ru1–P2 2.388(2), Ru1–N1 2.018(7), P1–Ru1–P2 92.49(8), P1–Ru1–N1 88.78(19), P2–Ru1–N1 87.38(18).

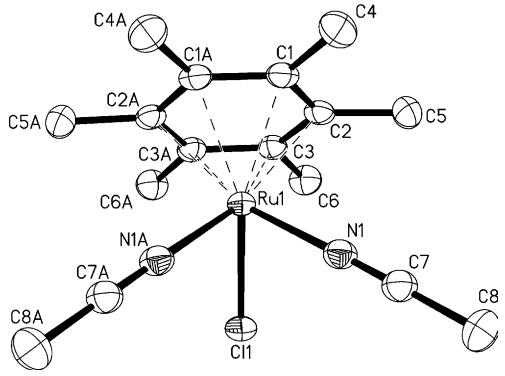


Fig. 4. Molecular structure of $[(HMB)Ru(CH_3CN)_2Cl]^+$ (**14** cation). Hydrogen atoms are omitted for clarity. Selected geometric parameters (Å, °): Ru1–Cl1 2.3975(8), Ru1–N1 2.072(2), N1–C7 1.1329(3), N1–Ru1–Cl1 85.22(6).

2-fold axis so that the ratio of complex to water is 1:1. The Ru atom in **5** also adopts a pseudo-octahedral geometry, being coordinated to a HMB ring, one P atom of a bridging dppf ligand and two N-bound thiocyanate ligands. The bonding mode of dppf in this structure contrasts with its chelating mode in the aforementioned structures of **1** and **2**. The Ru–N bond distances of 2.044(4) and 2.045(5) Å are shorter than that in **2** (2.076(3) Å) and the Ru–P bond distances of 2.3540(12) Å are the longest of these three structures. The overall structure for **5** is similar to that reported for $[(\eta^6\text{-}Me_4C_6H_2)RuCl_2]_2(\mu\text{-dppf})$ [10] allowing for differences in chemistry and the different crystallographic symmetry; the latter molecule is situated about a centre of inversion. The Ru atom is separated by 1.741(3) Å from the ring centroid of the HMB ligand. The dppf-Cp rings have an almost perfect *antiperiplanar staggered* conformation (P-ring centroid-P torsion angle is −176.1(2)°) in which the Fe atom is 1.647(2) Å from each of the ring centroids, the angle subtended at Fe by the ring centroids is 178.7(2)°, and the dihedral angle between the two Cp rings is 4.8(1)°.

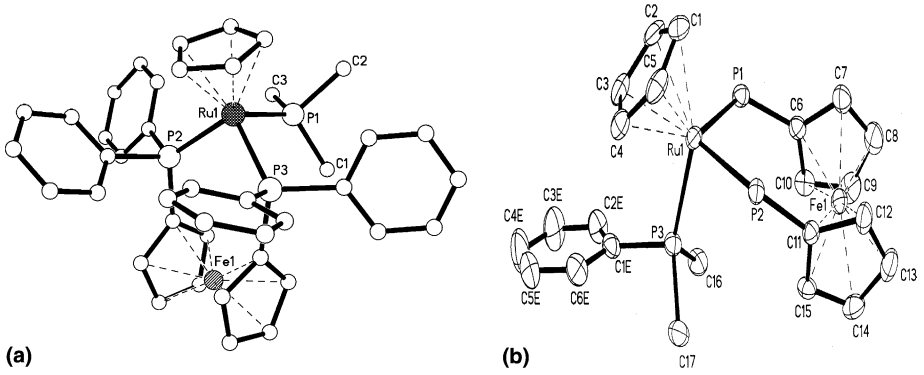


Fig. 5. (a) $[CpRu(dppf)(PMe_3)]^+$ (**8** cation). Hydrogen atoms are omitted for clarity. Selected geometric parameters (Å, °): Ru1–P1 2.3244(19), Ru1–P2 2.3399(18), Ru1–P3 2.357(2), P1–Ru1–P2 98.90(7), P1–Ru1–P3 94.42(7), P2–Ru1–P3 98.10(6). (b) Molecular structure of $[CpRu(dppf)(PMe_2Ph)]^+$ (**9** cation). Hydrogen atoms are omitted for clarity. Selected geometric parameters (Å, °): Ru1–P1 2.3436(11), Ru1–P2 2.3288(10), Ru1–P3 2.3432(10), P1–Ru1–P2 97.44(4), P1–Ru1–P3 97.64(4), P2–Ru1–P3 95.58(4).

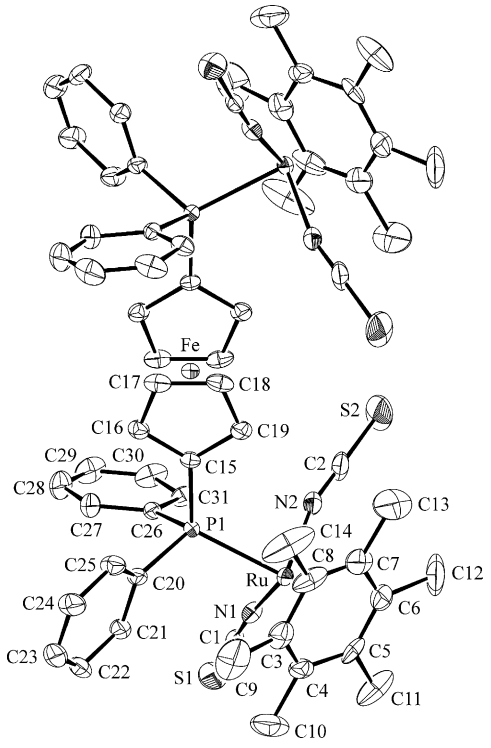


Fig. 6. Molecular structure of $[(HMB)Ru(NCS)_2]_2(\mu\text{-dppf})$ (**5**). Hydrogen atoms are omitted for clarity. Selected geometric parameters (Å, °): Ru–P1 2.3543(12), Ru–N1 2.044(4), Ru–N2 2.045(5), P1–Ru–N1 85.11(12), P1–Ru–N2 86.63(13), N1–Ru–N2 89.51(18), Ru–N1–C1 172.5(4), Ru–N2–C2 164.5(5), N1–C1–S1 178.0(5), N2–C2–S2 179.4(7).

The molecular structure of the diruthenium complex **11** (Fig. 7) shows the dithiocarbamate ligands chelated to the Ru center through two S donors, significantly different from the commonly monodentate mode in CpRu phosphine complexes, such as $[CpRu(L)_2(S_2CNEt_2)]$ synthesized by reactions of $[CpRu(L)_2Cl]$ ($L_2 = dppe$ or $L = PPh_3$) with sodium dithiocarbamate [21,32]. The dithiocarbamate ligands are in their usual $\eta^2$-chelate mode [33–35] with small bites (ca. 72°) at Ru. An important observation is that the bulky bridging dppf is relatively strongly coordinated to Ru (2.2616(11) and 2.2692(11) Å), the Ru–P bond lengths being significantly shorter than those of other CpRu(dppf) complexes (ca. 2.32 Å). In the formation of **11** from [CpRu(dppf)Cl], dppf has changed from $\eta^2$- to μ-bridging bonding mode, which does not happen with less bulky mono or diphosphines, e.g. in complex $[CpRu(dppe)(\eta^1\text{-}S_2CNEt_2)]$ (Scheme 5) [21]. Another feature of interest in **11** is the degree of double-bond character present in central C–N bond in the dithiocarbamate ligand, these bonds (C1–N1, C6–N2) exhibit partial double-bond character (1.339(6) and 1.333(6) Å), which could be found in the structure of $[CpRu(PPh_3)(\eta^2\text{-}S_2CNMe_2)]$ [32].

The molecular structure of the dication $[\{CpRu(dppf)\}_2(\mu\text{-}S_2)]^{2+}$ of **13** possessess ruthenium(III) centers linked by a disulfide bridge ($\mu\text{-}S_2^{2-}$), the Ru–S–S–Ru dihedral angle being 145.8°. (Fig. 8) Each sulfur, together with the chelating dppf and $\eta^5$-Cp, completes a piano-stool arrangement at the metal. The *syn*-$\eta^1$:$\eta^1$ mode adopted by the disulfide necessitates a *syn* arrangement of the two dppf, and the two $C_5$ rings, across the bridge. The interplanar angle between the Cp rings is 83.8°. The Ru–S bond lengths (2.330(2) and 2.334(2) Å) are in the normal range of Ru–S (2.30 Å) [36]. The S(1)–S(2) bond length 2.015(2) Å lies between the values for S=S in free $S_2$ (1.887 Å) [37] and S–S in $H_2S_2$ (2.055 Å) or $Me_2S_2$ (2.038 Å) [38,39]. Based on additional electrochemical and EPR data, Rauchfuss and co-workers [23a] had ascribed the short S–S bond (1.962(4) Å) and also short Ru–S bond (2.208(3) Å) in the analogous $[\{CpRu(PPh_3)_2\}_2(\mu_2\text{-}S_2)](SbF_6)_2$ complex to delocalized

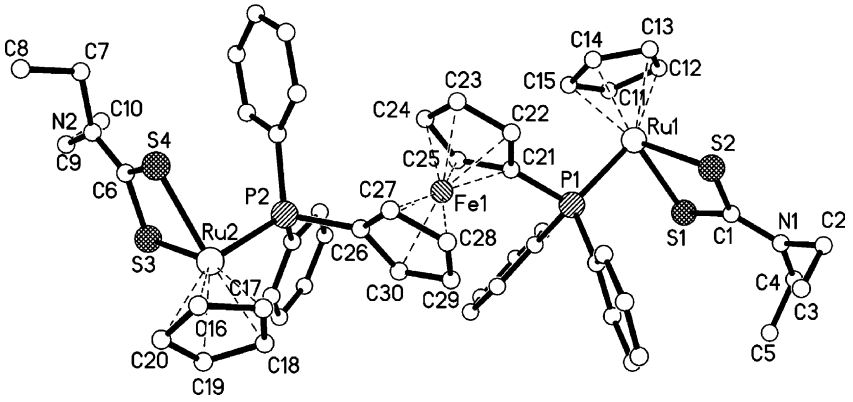


Fig. 7. Molecular structure of $[\{CpRu(S_2CNEt_2)\}_2(\mu\text{-dppf})]$ (**11**). Hydrogen atoms are omitted for clarity. Selected geometric parameters (Å, °): Ru1–P1 2.2616(11), Ru2–P2 2.2692(11), Ru1–S1 2.3926(12), Ru1–S2 2.3866(11), Ru2–S3 2.4072(13), Ru2–S4 2.3957(12), C1–N1 1.339(6), C6–N2 1.333(6), C2–N1 1.521(7), C1–S1 1.716(5), C1–S2 1.691(5), C6–S3 1.722(5), C6–S4 1.705(5), S1–Ru1–S2 72.17(4), S3–Ru2–S4 71.64(4), P1–Ru1–S1 89.88(4), P1–Ru1–S2 94.04(4), P2–Ru2–S3 86.17(4), P2–Ru2–S4 93.35(4), S1–C1–S2 111.4(3), S1–C1–N1 123.9(4), S2–C1–N1 124.5(4), S3–C6–S4 110.2(3), S3–C6–N2 124.4(4), S4–C6–N2 125.3(4).

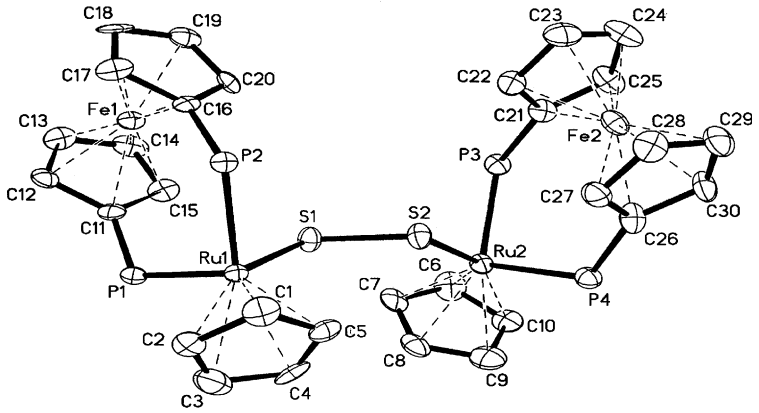


Fig. 8. Molecular structure of $[\{CpRu(dppf)\}_2(\mu_2\text{-}S_2)]^{2+}$ (**13** cation). Hydrogen atoms are omitted for clarity. Selected geometric parameters (Å, °): Ru1–S1 2.330(2), Ru2–S2 2.334(2), S1–S2 2.015(2), Ru1–P1 2.310(2), Ru1–P2 2.307(2), Ru2–P3 2.329(2), Ru2–P4 2.306(2), P1–Ru1–P2 97.76(6), P3–Ru2–P4 96.37(6), S1–Ru1–P1 89.73(6), S1–Ru1–P2 88.79(6), S2–Ru2–P3 89.25(6), S2–Ru2–P4 88.72(6), S1–S2–Ru2 108.31(8), S2–S1–Ru1 110.00(8).

π-bonding in the $Ru_2S_2$ core, facilitated by the strong π-donor capability of the $S_2$ ligand. It is noted that comparably short S–S bonds have been found in $[(\mu_2\text{-}S_2)(Cp^*Ru)_2(\mu_3\text{-}S)(\mu_2\text{-}S)_2MS]$ (M = W, Mo) (S–S 1.991(7) Å) by Hidai and co-workers [36], $[\{Ru^{III}(NH_3)_5\}_2(\mu\text{-}S_2)]Cl_4 \cdot 2H_2O$ (S–S 2.014(1) Å) by Elder and Trkula [40] and $[\{LRu(acac)\}_2(\mu\text{-}S_2)](PF_6)_2$ (L = 1,4,7-trimethyl-1,4,7-triazacyclononane, S–S 1.989(2) Å) by Wieghardt and co-workers [41].

## 3. Conclusions

With the donor ligands under investigation, [CpRu(dppf)Cl] (**1**) gives mononuclear chloro-substituted products, except in the reaction with $S_8$ which results in a $\mu\text{-}S_2$-bridged dinuclear species. With the same donor ligands, $[(HMB)Ru(dppf)Cl]PF_6$ (**3**) undergoes (i) chloride-only substitution with $CH_3CN$ or $NCS^-$, followed by further reaction of [(HMB)Ru(dppf)(NCS)]$PF_6$ (**4**) to form $[(HMB)Ru(NCS)_2]_2(\mu$-dppf) (**5**), (ii) arene cleavage with $S_2CNEt_2^-$, giving [Ru(dppf)$(S_2CNEt_2)_2$] (**12**), or (iii) dppf cleavage, resulting in $[(HMB)Ru(PMe_2Ph)_2Cl]PF_6$ (**10**) with $PMe_2Ph$ and $[(HMB)Ru(CH_3CN)_2Cl]PF_6$ (**14**) together with (dppf)$S_2$ with $S_8$. These reactions suggest that depending on synthetic conditions and ligand environment, one or several of the following can take place, viz, ligand substitution, anionic exchange, metal oxidation and ligand oxidation. The use of dppf as a supporting ligand introduces an additional dimension in the formation of dinuclear species. These coordination possibilities have prompted us to use this system for further synthetic investigations.

## 4. Experimental

### 4.1. General

All reactions were performed under dry nitrogen using Schlenk techniques. Solvents were freshly distilled from standard drying agents. $^1H$ and $^{31}P\{^1H\}$ NMR spectra were recorded on a Bruker ACF300 FT NMR spectrometer, with chemical shifts referenced to residual non-deutero solvent and external $H_3PO_4$, respectively. IR spectra were obtained a KBr disk on a Perkin–Elmer 1600 spectrophotometer. Mass spectra were obtained on a Finnigan MAT95XL-T spectrometer. All elemental analyses were performed in-house.

$RuCl_3 \cdot 3H_2O$ was obtained from Aldrich, and $PMe_3$, $PMe_2Ph$, $PPh_3$, dppf and $NaS_2CNEt_2$ from Merck. $[CpRu(PPh_3)_2Cl]$ [42], $[(HMB)RuCl_2]_2$ [43] and $[(HMB)Ru(dppf)Cl]PF_6$ [10] were prepared by published methods. All other reagents were obtained commercially.

### 4.2. Preparation of complexes

#### 4.2.1. [CpRu(dppf)Cl] (1)

Complex [CpRu(dppf)Cl] (**1**) was prepared from $[CpRu(PPh_3)_2Cl]$ and dppf according to the method of Bruce et al. [9], who obtained **1** after 16 h reflux in benzene.

A solution of $[CpRu(PPh_3)_2Cl]$ (0.369 g, 0.51 mmol) and dppf (0.306 g, 0.55 mmol) in toluene (30 ml) was heated under reflux for 12 h. Concentration of the solution followed by addition of hexane gave a bright-yellow solid of [CpRu(dppf)Cl] (**1**) which was washed twice with toluene and hexane (1:2, v/v) and ether, respectively, and dried in vacuo (0.301 g, 0.40 mmol, 78%

yield). Anal. Calc. for $C_{39}H_{33}ClP_2FeRu$: C, 62.0; H, 4.4; Cl, 4.7; P, 8.2. Found: C, 62.1; H, 4.3; Cl, 4.6; P, 8.3%. NMR ($CDCl_3$): $^1H$: $\delta$ 4.11 (s, 5H, $C_5H_5$), 4.03, 4.24, 4.32 and 5.19 (each s, total 8H, $C_5H_4$), 7.16 (s, 1H, Ph), 7.19 (s, 1H, Ph), 7.29–7.34 (m, 8H, Ph) and 7.39–7.45 (m, 10H, Ph); $^{31}P\{^1H\}$: $\delta$ 45.8 (s). NMR ($C_6D_6$): $^1H$: $\delta$ 4.16 (s, 5H, $C_5H_5$), $\delta$ 3.71, 3.94, 4.24 and 5.62 ($C_5H_4$ of dppf); $^{31}P\{^1H\}$: $\delta$ 46.2. $FAB^+$-MS: *m/z* 756 $[M]^+$, 721 $[M–Cl]^+$. IR (KBr, $cm^{-1}$): *v* 1433, 1090, 695, 514, 505 and 479.

A subsequent reaction showed that the reaction was complete after 4 h in refluxing toluene.

#### 4.2.2. [CpRu(dppf)(NCS)] (2)

To a yellow suspension of **1** (0.037 g, 0.05 mmol) in MeOH (5 ml), NaNCS (0.008 g, 0.10 mmol) was added and the mixture was stirred for 6 h. The resultant yellow suspension was filtered to collect the yellow precipitate of [CpRu(dppf)(NCS)] (**2**), which was washed with MeOH ($2 \times 2$ ml) and ether ($2 \times 2$ ml) and dried in vacuo (0.031 g, 0.04 mmol, 80% yield). Anal. Calc. for $C_{40}H_{33}NP_2SFeRu$: C, 61.7; H, 4.3; S, 4.1. Found: C, 61.7; H, 4.35; S, 4.2%. NMR ($CDCl_3$, 300 K): $^1H$: $\delta$ 4.30 (s, 5H, $C_5H_5$), 4.08, 4.12, 4.26 and 4.35 (each s, 2H, $C_5H_4$), 7.35 and 7.63 (each c.m, total 20H, Ph); $^{31}P\{^1H\}$: $\delta$ 48.6 (s). $FAB^+$-MS: *m/z* 779 $[M]^+$, 721 $[M–NCS]^+$, 1499 $[2M–NCS]^+$. IR (KBr, $cm^{-1}$): *v*(C≡N) 2105s, *v*(C–S) 697s.

#### 4.2.3. [(HMB)Ru(dppf)(NCS)]$PF_6$ (4) and [(HMB)Ru(NCS)$_2$]$_2$μ-dppf) (5)

A mixture of [(HMB)Ru(dppf)Cl]$PF_6$ (**3**) (68 mg, 0.07 mmol) and NaNCS (6 mg, 0.07 mmol) was refluxed in MeOH (10 ml) for 23 h, resulting in an orange yellow suspension. The solids [(HMB)Ru(dppf)(NCS)]$PF_6$ (**4**) were filtered, washed with MeOH and ether and dried in vacuo. The filtrate was evacuated to dryness, extracted with $CH_2Cl_2$ ($5 \times 2$ ml). The combined extracts were filtered to remove sodium salt. The residue was recrystallized in $CH_2Cl_2$-hexane (1:4) to give an orange solid of **4** (total yield, 63 mg, 0.06 mmol, 88%). Anal. Calc. for $C_{47}H_{46}F_6NP_3SFeRu$: C, 55.3; H, 4.5; N, 1.4; S, 3.1. Found: C, 55.4; H, 4.6; N, 1.3; S, 3.4%. NMR ($CDCl_3$, 300 K): $^1H$: $\delta$ 1.58 (s, 18H, $C_6Me_6$), 4.04, 4.11, 4.35 and 4.76 (each s, total 8H, $C_5H_4$), 7.33, 7.51 and 7.67 (each c.m, unres., total 20H, Ph); $^{31}P\{^1H\}$: $\delta$ 38.4 (s, dppf), −144 ($PF_6$). $FAB^+$-MS: *m/z* 876 $[M]^+$, 818 $[M–SCN]^+$, 714 $[M–C_6Me_6]^+$, 655 $[M–C_6Me_6–SCN]^+$. $FAB^-$-MS: *m/z* 145 $[PF_6]^-$. IR (KBr, $cm^{-1}$): *v*(C≡N) 2100 vs, *v*(C–S) 698m, *v*($PF_6$) 813s, 474m.

A similar mixture of [(HMB)Ru(dppf)Cl]$PF_6$ (**3**) (30 mg, 0.03 mmol) and excess NaNCS (5 mg, 0.07 mmol) in $CH_3CN$ (25 ml) was stirred for 2–3 days. A yellow suspension resulted. The mixture was filtered to remove a yellow precipitate of displaced dppf, diagnosed via $^1H$ and $^{31}P\{^1H\}$ NMR spectra. The filtrate was concentrated to ca. 2 ml and ether (3 ml) added; after 1 h at 0–5 °C, yellow solids of [(HMB)Ru(NCS)$_2$]$_2$(μ-dppf) (**5**) (13 mg, 0.01 mmol, 67%) were obtained. Anal. Calc. for $C_{62}H_{64}N_4P_2S_4FeRu_2$: C, 56.7; H, 4.9; N, 4.3; S, 9.8. Found: C, 56.7; H, 4.8; N, 4.2; S, 9.8%. NMR ($CDCl_3$, 300 K): $^1H$: $\delta$ 1.77 (s, 36H, $C_6Me_6$), 4.10 (c.m, unres., 8H, $C_5H_4$), 7.50 (c.m with a sharp signal at $\delta$ 7.41, 20H, Ph); $^{31}P\{^1H\}$: $\delta$ 27.3 (s). $FAB^+$-MS: *m/z* 701 $[M–NCS–dppf]^+$. (KBr, $cm^{-1}$): *v*(C≡N) 2106 vs, *v*(C–S) 699m.

Likewise, a mixture of [(HMB)Ru(NCS)]$PF_6$ (**4**) (15 mg, 0.02 mmol) and NaNCS (5 mg, 0.06 mmol) in $CH_3CN$ (20 ml) was stirred for 2 days. A yellow suspension was resulted. The mixture was filtered to remove a yellow precipitate of displaced dppf, diagnosed via $^1H$ and $^{31}P\{^1H\}$ NMR spectra. The filtrate was concentrated to ca. 1 ml and ether (2 ml) added; after 3 h at 0 °C, yellow solids were collected (9 mg, 0.007 mmol, 70%). Its NMR resonance of dppf and HMB, FAB and IR spectra are identical to those of **5**.

#### 4.2.4. [CpRu(dppf)($CH_3CN$)]$BPh_4$ (6) and [(HMB)Ru(dppf)($CH_3CN$)]($PF_6$)$_2$ (7)

A reaction of **1** (0.020 g, 0.03 mmol) in $CH_3CN$ (20 ml) with $NaBPh_4$ (0.035 g, 1 mmol) for 1 h gave orange solids of [CpRu(dppf)($CH_3CN$)]$BPh_4$ (**6**) (0.036 g, 0.03 mmol, 80% yield). Anal. Calc. for $C_{65}H_{56}BNP_2FeRu$: C, 72.2; H, 5.2; N, 1.3. Found: C, 72.9; H, 5.2; N, 1.4%. NMR ($CDCl_3$): $^1H$: $\delta$ 2.29 (s, $CH_3CN$), 4.30, 4.36 (each s, total 8H, $C_5H_4$), 4.39 (s, 5H, $C_5H_5$), 7.41–7.80 (m, 40H, Ph); $^{31}P\{^1H\}$: $\delta$ 46.1 (s). $ESI^+$-MS: *m/z* 761 $[M]^+$, 721 $[M–CH_3CN]^+ \cdot$ $ESI^-$-MS: *m/z* 319 $[BPh_4]^-$. IR (KBr, $cm^{-1}$): *v*(C≡N) 2259.

A mixture of [(HMB)Ru(dppf)Cl]$PF_6$ (**3**) (30 mg, 0.03 mmol) and $NH_4PF_6$ (10 mg, 0.06 mmol) in $CH_3CN$ (25 ml) was refluxed for 24 h. The orange suspension was filtered through celite. Concentration of the filtrate to ca. 2 ml, followed by addition of ether (3 ml) and cooling at 0–5 °C for 1 h gave orange solids of [(HMB)Ru(dppf)($CH_3CN$)]($PF_6$)$_2$ (**7**) (21 mg, 0.02 mmol, 62%). Anal. Calc. for $C_{48}H_{49}F_{12}NP_4FeRu$. C, 50.2; H, 4.3; N, 1.2. Found: C, 50.3; H, 4.4; N, 1.2%. $^1H$ NMR ($CDCl_3$): $\delta$ 1.60 (s br, 18H, $C_6Me_6$), 2.22 (s, 3H, $CH_3CN$), 3.97, 4.09, 4.24 and 4.94 (each s, total 8H, $C_5H_4$), 7.42, 7.54, 7.71 and 7.82 (each s br, total 20H, Ph). $^{31}P\{^1H\}$ NMR ($CDCl_3$): $\delta$ 34.2 (s, dppf), −144 (septet, $PF_6$). $FAB^+$-MS: *m/z* 655 $[M–C_6Me_6\text{-}CH_3CN]^+$ and unassignable mass fragments 693 and 855. IR (KBr, $cm^{-1}$): *v*(C≡N) 2363s, *v*($PF_6$) 834s and 556s.

#### 4.2.5. [CpRu(dppf)(L)]$PF_6$ (L = $PMe_3$ (8), $PMe_2Ph$ (9)) and [(HMB)Ru($PMe_2Ph_2$)$_2$Cl]$PF_6$ (10)

A reaction of **1** (0.057 g, 0.08 mmol) with $PMe_3$ (0.1 ml, 0.11 mmol) and $NH_4PF_6$ (0.017 g, 0.1 mmol) in MeOH (10 ml) gave yellow solids of [CpRu(dppf)($PMe_3$)]$PF_6$ (**8**) (0.059 g, 0.06 mmol, 84%

yield). Anal. Calc. for $C_{42}H_{42}F_6P_4FeRu \cdot CH_2Cl_2$: C, 50.3; H, 4.3; F, 11.1; P, 12.0. Found: C, 50.0; H, 4.3; F, 12.0; P, 12.1%. NMR ($CDCl_3$): $^1H$: 1.39 (d, 9H, $PMe_3$); 4.38 and 4.51 (each s, 4H, $C_5H_4$); 4.75 (s, 5H, $C_5H_5$); 7.26–7.42 (m, 20H, Ph); $^{31}P\{^1H\}$: $\delta$ 49.8 (d, $J(PP) = 42$ Hz, dppf); −10.1 (t, $J(PP) = 42$ Hz, $PMe_3$); −144 (septet, $J(PF) = 710$ Hz, $PF_6$). IR (KBr, $cm^{-1}$): $\nu(PF_6)$ 841s, 556s. $FAB^+$-MS: *m/z* 797 $[M]^+$, 721 $[M–PMe_3]^+$. $FAB^-$-MS: *m/z* 145 $[PF_6]^-$.

Likewise, a reaction of **1** (0.061 g, 0.08 mmol) with $PMe_2Ph$ (0.015 ml, 0.1 mmol) and $NH_4PF_6$ (0.018 g, 0.11 mmol) in MeOH (20 ml) gave yellow solids of $[CpRu(dppf)(PMe_2Ph)]PF_6$ (**9**) (0.068 g, 0.07 mmol, 85% yield). Anal. Calc. for $C_{47}H_{44}F_6P_4FeRu$: C, 56.2; H, 4.4; F, 11.4; P, 12.3. Found: C, 56.0; H, 4.7; F, 11.2; P, 11.9%. NMR ($CDCl_3$): $^1H$: $\delta$ 1.66 (d, 6H, $PMe_2Ph$); 4.45 (s, 5H, $C_5H_5$); 4.31, 4.38, 4.60 and 4.68 (each s, total 8H, $C_5H_4$); 7.09, 7.33 and 7.39 (each, c.m, total 25H, Ph); $^{31}P\{^1H\}$: $\delta$ 48.7 (d, $J(PP) = 42$ Hz, dppf); 0.6 (t, $J(PP) = 42$ Hz, $PMe_2Ph$); −144 (septet, $J(PF) = 713$ Hz, $PF_6$). IR (KBr, $cm^{-1}$): $\nu(PF_6)$ 839s, 556s. $FAB^+$-MS: *m/z* 859 $[M]^+$, 721 $[M–PMe_3]^+$. $FAB^-$-MS: 145 $[PF_6]^-$.

To a solution of **3** (30 mg, 0.03 mmol) in $CH_3CN$ (10 ml) was added $PMe_2Ph$ (4 μl, 0.03 mmol) and the mixture was stirred for 8 h. A yellow suspension was resulted. The yellow precipitate, found to be free dppf, was filtered off. The orange filtrate on concentration to ca. 3 ml gave orange red crystals of $[(HMB)Ru(PMe_2Ph)_2Cl]PF_6$ (**10**) (13 mg, 60%). Anal. Calc. of $C_{28}H_{40}ClF_6P_3Ru$: C, 46.7; H, 5.6; P, 12.9. Found: C, 46.5; H, 5.6; P, 12.0%. $^1H$ NMR ($CDCl_3$): $\delta$ 1.67 (s, 18h, $C_6Me_6$), 1.92 (d, $J = 6$ Hz, 12H, $PMe_2Ph$), 7.49–7.71 (m, 10H, Ph). $^{31}P\{^1H\}$ NMR ($CDCl_3$): $\delta$ 6.6 (s, $PMe_2Ph$), −144 (septet, $PF_6$). $FAB^+$-MS: *m/z* 575 $[M]^+$. IR (KBr, $cm^{-1}$): $\nu(PF_6)$ 841s, 557s.

#### 4.2.6. *[{CpRu(S$_2$CNEt$_2$)}$_2$(μ-dppf)] (**11**) and [Ru(dppf)(S$_2$CNEt$_2$)$_2$] (**12**)*

A yellow suspension of **1** (0.064 g, 0.08 mmol) and sodium diethyldithiocarbamate (0.024 g, 0.11 mmol) in MeOH (20 ml) was heated under reflux for 10 h. The resultant orange suspension was filtered to collect the orange precipitates of $[\{CpRu(S_2CNEt_2)\}_2(\mu\text{-dppf})]$ (**11**), which were washed twice with methanol and ether and dried in vacuo. Recrystallization in $CH_2Cl_2$/hex gave orange crystals (0.030 g, 0.025 mmol, 60% yield) after 1 h at 0 °C. Anal. Calc. for $C_{54}H_{58}N_2P_2S_4FeRu_2 \cdot CH_2Cl_2$: C, 52.1; H, 4.8; N, 2.2; P, 4.9; S, 10.1. Found: C, 52.2; H, 4.6; N, 2.2, P, 4.5; S, 10.0%. NMR ($CDCl_3$): $^1H$: $\delta$ 0.91 (t, $J = 7$ Hz, 12H, $CH_3$), 3.23 (q, unres., 8H, $CH_2$), 4.20 and 4.09 (each s, total 8H, $C_5H_4$), 4.47 (s, 5H, $C_5H_5$), 7.18 and 7.47 (each c.m, total 20H, $C_6H_5$); $^{31}P\{^1H\}$: $\delta$ 47.5 (s). $FAB^+$-MS: *m/z* 1180 $[M]^+$, 869 $[CpRu(dppf)(S_2CNEt_2)]^+$, 721 $[CpRu(dppf)]^+$, 554 $[dppf]^+$. IR (KBr, $cm^{-1}$): $\nu$(CN) 1486m; $\nu(NC_2)$ 1146m; (CS) 792m; $\nu$(others) 2971w, 2928w, 2374w, 2336w, 1647wbr, 1430m, 1268s, 1090s, 1028s, 685s, 534msh, 469s.

A mixture of **3** (29.4 mg, 0.03 mmol) and $NaS_2CNEt_2.3H_2O$ (9.1 mg, 0.04 mmol) was refluxed for 24 h in MeOH (15 ml). The yellow solids of $[Ru(S_2CNEt_2)_2(dppf)]$ (**12**) were filtered, washed with MeOH and ether, and evacuated to dryness (5 mg, 0.005 mmol, 26%). Anal. Calc. for $C_{44}H_{48}N_2P_2S_2FeR$: C, 55.5; H, 5.1; N, 2.9. Found: C, 54.7; H, 5.4; N, 2.6%. $^1H$ NMR ($CDCl_3$): $\delta$ 0.98 (s, $v_{1/2}$18 Hz, 12H, $CH_3$), 3.24 (s, $v_{1/2} = 42$ Hz, 2H, $CH_2$), 3.53 (s, $v_{1/2} = 33$ Hz, 6H, $CH_2$), 4.20 (s, 2H, $C_5H_4$), 4.36 (s, 2H, $C_5H_4$), 4.44 (s, 4H, $C_5H_4$), 7.17 and 7.24 (overlapping triplets, $J = 7$ Hz, 12 H, Ph), 7.68 (s, $v_{1/2} = 26$ Hz, 8H, Ph). $^{31}P\{^1H\}$ NMR ($CDCl_3$): $\delta$ 47.7 (s, dppf). $FAB^+$-MS: *m/z* 952 $[M]^+$, 804 $[M\text{-}(S_2CNEt_2)]^+$. IR (KBr, $cm^{-1}$): $\nu$(CN) 1485m; $\nu(NC_2)$ 1144m; $\nu$(CS) 695m; $\nu$(others) 3052w, 2966w, 2923w, 2869vw, 1428m, 1360w, 1271m, 1214vw, 1082m, 1030m, 905vw, 810w, 744w. Free HMB ligand was diagnosed by $^1H$ NMR and $FAB^+$-MS.

#### 4.2.7. *[{CpRu(dppf)}$_2$(μ-S$_2$)](BPh$_4$)Cl (**13**) and [(HMB)Ru(CH$_3$CN)$_2$Cl]PF$_6$ (**14**)*

To a yellow solution of **1** (0.053 g, 0.07 mmol) in $CH_2Cl_2$ (10 ml), $NaBPh_4$ (0.086 g, 0.25 mmol) and elemental sulfur (0.017 g, 0.52 mmol) were added and the mixture was stirred for 9 h. The deep green resultant suspension solution was filtered to remove the sodium salts. The filtrate was evacuated to dryness and the solids extracted with toluene to remove excess sulfur and unreacted **1**. The residue was dissolved in ca. 2 ml of acetone and hexane was added, giving deep green solids of $[\{CpRu(dppf)\}_2(\mu_2\text{-}S_2)](BPh_4)Cl$ (**13**) (0.045 g, 0.024 mmol, 69% yield). Anal. Calc. for $C_{102}H_{86}BClFe_2P_4Ru_2S_2$: C, 65.9; H, 4.7; B, 0.6; Cl, 1.9; S, 3.5. Found: C, 65.5; H, 5.1; B, 1.2; Cl, 1.5; S, 3.1%. NMR ($CDCl_3$): $^1H$: $\delta$ 4.07 (vbr, $v_{1/2}$ ca. 60 Hz, 26H, $C_5H_5$ and $C_5H_4$), 6.86 (s, br), 7.02 (s, br) and 7.42–7.57 (m, total, ca. 60H, Ph). $^{31}P\{^1H\}$ NMR ($CDCl_3$): no signal. $FAB^+$-MS: *m/z* 1506 $[M]^+$, 721 $[CpRu(dppf)]^+$. $FAB^-$-MS: *m/z* 319 $[BPh_4]^-$. IR (KBr, $cm^{-1}$): $\nu$ 3058w, 2924w, 2362w, 2342w, 1478m, 1432m, 1159msh, 1089s, 1032m, 804m, 745s, 698vs, 621w, 508vs, 470s, 438m.

To a solution of **3** (64 mg, 0.06 mmol) in $CH_3CN$ (10 ml) was added $S_8$ (16 mg, 0.5 mmol S) and the mixture was stirred for 4 h. A yellow suspension was resulted. The yellow solids of $dppfS_2$ [34] were removed by filtration. Concentration of the orange filtrate to ca. 3 ml gave orange red crystals of $[(HMB)Ru(CH_3CN)_2Cl]PF_6$ (**14**) (10 mg, 63%). Anal. Calc. of $C_{16}H_{24}ClF_6N_2PRu$: C, 36.5; H, 4.6; N, 5.3. Found: C, 36.5; H, 4.5; N, 5.4%. $^1H$ NMR ($CD_3CN$): $\delta$ 2.13 ($C_6Me_6$). $FAB^+$-MS: *m/z* 381 $[M]^+$, 340 $[M–CH_3CN]^+$. $FAB^-$-MS: 145 $[PF_6]^-$. IR (KBr, $cm^{-1}$): $\nu(C{\equiv}N)$ 2359m, $\nu(PF_6)$ 841s, 557s.

Table 1
Crystal and structure refinement data for **1**, **2** · acetone, **5** · $H_2O$, **6**, **7**, **8**, **9**, **11** · $CH_2Cl_2$, **13** and **14**[a]

| Complexes | **1** | **2** · acetone | **5** · $H_2O$ | **6** | **7** · 0.5$CH_3CN$ | **8** · 0.5$Et_2O$ | **9** | **11** · $CH_2Cl_2$ | **13** · 3.5$CH_3CN$ | **14** |
|---|---|---|---|---|---|---|---|---|---|---|
| Empirical formula | $C_{39}H_{33}ClFeP_2Ru$ | $C_{43}H_{39}FeNOP_2RuS$ | $C_{62}H_{66}FeN_4OP_2Ru_2S_4$ | $C_{65}H_{56}BFeP_2Ru$ | $C_{49}H_{50.50}F_{12}FeN_{1.50}P_4Ru$ | $C_{44}H_{47}F_6FeO_{0.50}P_4Ru$ | $C_{47}H_{44}F_6FeP_4Ru$ | $C_{55}H_{60}Cl_2FeN_2P_2Ru_2S_4$ | $C_{109}H_{96.50}BClFe_2N_{3.50}P_4Ru_2S_2$ | $C_{16}H_{24}ClF_6N_2PRu$ |
| Formula weight | 755.96 | 836.67 | 1321.34 | 1080.78 | 1169.21 | 978.62 | 1003.62 | 1268.12 | 2003. 50 | 525.86 |
| Space group | $P2_1/c$ | $P2_1/c$ | $C2/c$ | $P1$ | $P2/c$ | *Pbca* | $P2_1/n$ | $P\bar{1}$ | $P\bar{1}$ | $P2_1$ |
| Crystal system | Monoclinic | Monoclinc | Monoclinic | Triclinic | Monoclinic | Orthorhombic | Monoclinic | Triclinic | Triclinic | Monoclinic |
| $a$ (Å) | 13.5991(7) | 10.9200(7) | 33.812(4) | 11.3484(5) | 19.402(7) | 20.0967(12) | 13.5735(18) | 10.3688(7) | 14.5687(12) | 7.5406(4) |
| $b$ (Å) | 14.1731(7) | 22.5250(16) | 10.7494(11) | 13.8966(6) | 10.967(4) | 16.3787(9) | 21.673(3) | 15.8105(11) | 17.4655(15) | 10.8604(6) |
| $c$ (Å) | 16.1793(8) | 15.0620(11) | 16.8236(18) | 16.7462(7) | 23.112(8) | 27.1174(16) | 14.791(2) | 18.1584(12) | 20.9156(18) | 12.4754(7) |
| $\alpha$ (°) | 90 | 90 | 90 | 80.0980(10) | 90 | 90 | 90 | 101.1610(10) | 86.325(2) | 90 |
| $\beta$ (°) | 95.348(2) | 91.239(2) | 105.383(2) | 82.6470(10) | 104.957(9) | 90 | 96.706(3) | 102.8270(10) | 72.933(2) | 96.9350(10) |
| $\gamma$ (°) | 90 | 90 | 90 | 84.5570(10) | 90 | 90 | 90 | 106.1020(10) | 73.770(2) | 90 |
| $V$ (Å$^3$) | 3104.8(3) | 3704.0(4) | 5895.7(11) | 2573.03(19) | 4751(3) | 8925.9(9) | 4321.3(10) | 2683.2(3) | 4883.9(7) | 1014.18(10) |
| Z | 4 | 4 | 4 | 2 | 4 | 8 | 4 | 2 | 2 | 2 |
| $D_{calc}$ (g cm$^{-3}$) | 1.617 | 1.500 | 1.489 | 1.395 | 1.635 | 1.456 | 1.543 | 1.570 | 1.362 | 1.722 |
| $\mu$ (mm$^{-1}$) | 1.172 | 0.978 | 0.988 | 0.681 | 0.843 | 0.863 | 0.893 | 1.176 | 0.779 | 1.040 |
| Crystal size (mm) | 0.04 × 0.14 × 0.20 | 0.21 × 0.21 × 0.42 | 0.30 × 0.10 × 0.08 | 0.4 × 0.2 × 0.2 | 0.18 × 0.18 × 0.09 | 0.1× 0.04 × 0.04 | 0.24 × 0.18 × 0.04 | 0.36 × 0.14 × 0.08 | 0.2 × 0.15 × 0.05 | 0.40 × 0.40 × 0.26 |
| $\theta$ Range for data collection (°) | 1.0–30.0 | 1.6–30.0 | 1.99–25.00 | 1.49–30.04 | 1.82–25.00 | 1.81–25.00 | 1.78–30.07 | 1.20–25.00 | 1.52–25.00 | 1.64–27.50 |
| Data/restraints/ parameters | 8838/0/397 | 10 762/0/433 | 5183/0/347 | 14 590/0/641 | 8359/825/611 | 7855/91/506 | 12 128/0/534 | 9459/0/617 | 17 215/15/1095 | 2421/0/178 |
| Goodness-of-fit on $F^2$ | 1.00 | 1.08 | 1.088 | 0.998 | 0.828 | 1.055 | 1.042 | 1.058 | 1.122 | 1.073 |
| Final $R$ indices $[I > 2\sigma(I)]$ | $R_1 = 0.069$; $\omega R_2 = 0.120$ | $R_1 = 0.049$; $\omega R_2 = 0.130$ | $R_1 = 0.0482$; $\omega R_2 = 0.1134$ | $R_1 = 0.0401$; $\omega R_2 = 0.0816$ | $R_1 = 0.0633$; $\omega R_2 = 0.1355$ | $R_1 = 0.0594$; $\omega R_2 = 0.1269$ | $R_1 = 0.0505$; $\omega R_2 = 0.0899$ | $R_1 = 0.0490$; $\omega R_2 = 0.1130$ | $R_1 = 0.0916$; $\omega R_2 = 0.1840$ | $R_1 = 0.0307$; $\omega R_2 = 0.0817$ |

[a] Temperature for analyses = 223 K; wavelength for analysis = 0.71073 Å.

### 4.3. X-ray diffraction analyses

Diffraction-quality single crystals of **1** were obtained from $CH_2Cl_2$ layered with hexane, **2** · acetone from acetone layered with ether and **5** · $H_2O$ from a $CHCl_3$ solution layered with hexane after 1–5 days at ambient temperature, **6**, **7**, **13** and **14** from $CH_3CN$ solutions layered with ether after 3 days at −29 °C, **8** and **9** from a solution in MeOH and ether after 3 h at 0 °C and **11** from a solution in $CH_2Cl_2$ and hexane after 1 h at 0 °C.

X-ray data were collected on a Bruker AXS SMART CCD diffractometer using Mo Kα radiation at 223 K so that $\theta_{max}$ was 30.0°. Data were reduced (SMART & SAINT [44]) and corrected for absorption effects (SADABS [45]). The structures were solved by heavy-atom methods using SHELXS [46] (PATTY in DIRDIF [47] for **2**) and refined (anisotropic displacement parameters (except for solvent molecules), H atoms in calculated positions (except for water molecule in **5**), and a weighting scheme of the form $w = 1/[\sigma^2(F_o^2) + aP^2 + bP]$, where $P = (F_o^2 + 2F_c^2)/3$) on $F^2$ (SHELX-97 [48]). Crystallographic data are summarized in Table 1 and the molecular structures are shown in Figs. 1–8. Data manipulation was conducted with teXsan [49].

## 5. Supplementary material

Crystallographic data for **1**, **2**, **5–9**, **11**, **13** and **14** have been deposited at the Cambridge Crystallographic Data Centre with deposition numbers 213731–213733, 221835–221841, respectively. Copies of the information may be obtained free of charge from The Director, CCDC, 12 Union Road, Cambridge CB2 1EZ, UK (Fax: +44-1223-336033; e-mail: deposit@ccdc.cam.ac.uk or www: http://www.ccdc.cam.ac.uk).

## Acknowledgements

Support from the National University of Singapore (Grant Nos. RP-143-000-77-112 and RP-143-000-135-112) to L.Y.G. and a research scholarship to X.L.L. are gratefully acknowledged.

## References

[1] S.G. Davies, J.P. McNally, A.J. Smallridge, in: F.G.A. Stone, R. West (Eds.), Advances in Organometallic Chemistry, vol. 30, 1990, p. 1, and references therein.
[2] T. Blackmore, M.I. Bruce, F.G.A. Stone, J. Chem. Soc. A (1971) 2376.
[3] (a) See for instance: H. Le Bozec, D. Touchard, P.H. Dixneuf, in: F.G.A. Stone, R. West (Eds.), Advances in Organometallica Chemistry, vol. 29, 1989, p. 163, and references therein;
(b) M.A. Bennett, L.Y. Goh, I.J. McMahon, T.B.R. Mitchell, G.B. Robertson, T.W. Turney, W.A. Wickramasinghe, Organometallics 11 (1992) 3069, and references therein;
(d) D.E. Fogg, B.R. James, J. Organomet. Chem. 462 (1993) C21, and references therein;
(e) M.A. Bennett, K. Khan, E. Wenger, in: E.W. Abel, F.G.A. Stone, G. Wilkinson (Eds.), Comprehensive Organometallic Chemistry, vol. II, 1995, p. 473, Chapter 8, and references therein.
[4] M. Tokunaga, T. Suzuki, N. Koga, T. Fukushima, A. Horiuchi, Y. Wakatsuki, J. Am. Chem. Soc. 123 (2001) 11917.
[5] Y. Watanabe, T. Ando, M. Kamigaito, M. Sawamoto, Macromolecules 34 (2001) 4370.
[6] K.-S. Tan, T.S.A. Hor, in: A. Togni, T. Hayashi (Eds.), Ferrocenes – Homogeneous Catalysis, Organic Synthesis and Material Science, VCH, Weinheim, 1995, p. 3.
[7] G. Bandoli, A. Dolmella, Coord. Chem. Rev. 209 (2000) 161.
[8] R.T. Hembre, J.S. McQueen, V.W. Day, J. Am. Chem. Soc. 118 (1996) 798.
[9] M.I. Bruce, I.R. Butler, W.R. Cullen, G.A. Koustanonis, M.R. Snow, E.R.T. Tieknik, Aust. J. Chem. 41 (1988) 963.
[10] J.-F. Ma, Y. Yamamoto, J. Organomet. Chem. 560 (1998) 223.
[11] S.B. Jensen, S.J. Rodger, M.D. Spicer, J. Organomet. Chem. 556 (1998) 151.
[12] I.-Y. Wu, J.T. Lin, J. Luo, S.-S. Sun, C.-S. Li, K.J. Lin, C. Tsai, C.-C. Hsu, J.-L. Lin, Organometallics 16 (1997) 2038.
[13] S. Hartmann, R.F. Winter, B.M. Brunner, B. Sarkar, A. Knödler, I. Hartenbach, Eur. J. Inorg. Chem. (2003) 876.
[14] M. Sato, M. Asai, J. Organomet. Chem. 508 (1996) 121.
[15] V.W.-W. Yam, V.W.-M. Lee, K.-K. Cheung, J. Chem. Soc., Dalton Trans. (1997) 2335.
[16] A. Santos, J. López, J. Montoya, P. Noheda, A. Romero, A.M. Echavarren, Organometallics 13 (1994) 3605.
[17] S.-H. Han, K.-M. Sung, S. Hun, M.-J. Jun, D. Whang, K. Kim, Polyhedron 15 (1996) 3811.
[18] N.W. Alcock, J.M. Brown, M. Rose, A. Wienand, Tetrahedron: Asymm. 2 (1991) 47.
[19] H. Kawano, Y. Nishimura, M. Onishi, J. Chem. Soc., Dalton Trans. (2003) 1808.
[20] See for instance the following: (a) M.A. Bennett, T.W. Matheson, G.B. Robertson, W.L. Steffen, T.W. Turney, J. Chem. Soc., Chem. Commun. (1979) 32;
(b) T.P. Gill, K.R. Mann, Organometallics 1 (1982) 485;
(c) P.J. Fagan, M.D. Ward, J.C. Calabrese, J. Am. Chem. Soc. 111 (1989) 1698;
(d) F.B. McCormick, D.D. Cox, W.B. Gleason, Organometallics 13 (1993) 610;
(e) M.A. Bennett, L.Y. Goh, A.C. Willis, J. Am. Chem. Soc. 118 (1996) 4984;
(f) B. Steinmetz, W.A. Schenk, Organometallics 18 (1999) 943;
(g) L.Y. Goh, M.E. Teo, S.B. Khoo, W.K. Leong, J.J. Vittal, J. Organomet. Chem. 664 (2002) 161.
[21] A. Coto, M.J. Tenorio, M.C. Puerta, P. Valerga, Organometallics 17 (1998) 4392.
[22] X.L. Lu, S.Y. Ng, J.J. Vittal, G.K. Tan, L.Y. Goh, T.S.A. Hor, J. Organomet. Chem. 688 (2003) 100.
[23] (a) J. Amarasekera, T.B. Rauchfuss, S.R. Wilson, Inorg. Chem. 26 (1987) 3328;
(b) J. Amarasekera, T.B. Rauchfuss, Inorg. Chem. 28 (1989) 3875.
[24] Z.-G. Fang, T.S.A. Hor, Y.-S. Wen, L.-K. Liu, T.C.W. Mak, Polyhedron 17 (1995) 2403.
[25] J.J. Bishop, A. Davison, M.L. Katcher, D.W. Lichtenberg, R.E. Merrill, J.C. Smart, J. Organomet. Chem. 27 (1971) 241.
[26] K.M. Rao, L. Mishra, U.C. Agarwala, Polyhedron 6 (1987) 1383.

[27] M.K. Nazeeruddin, S.M. Zakeeruddin, R. Humphry-Baker, M. Jirousek, P. Liska, N. Vlachopoulos, V. Shklover, C.-H. Fischer, M. Grätzel, Inorg. Chem. 38 (1999) 6298.
[28] H. Nagao, D. OoYama, T. Hirano, H. Naoi, M. Shimada, S. Sasaki, N. Nagao, M. Mukaida, T. Oi, Inorg. Chim. Acta 320 (2001) 60.
[29] S. Suravajjala, L.C. Porter, Acta Crystallogr., Sect. C 49 (1993) 1456.
[30] W.H. Pearson, J.E. Shade, J.E. Brown, T.E. Bitterwolf, Acta Crystallogr., Sect. C 52 (1996) 1106.
[31] S.J. Simpson, Acta Crystallogr., Sect. C 48 (1992) 544.
[32] Q.J. McCubbin, F.J. Stoddart, T. Welton, A.J.P. White, D.J. Williams, Inorg. Chem. 37 (1998) 3753.
[33] A.N. Bhat, R.C. Fay, D.F. Lewis, A.F. Lindmark, S.H. Strauss, Inorg. Chem. 13 (1974) 886.
[34] C.L. Raston, A.H. White, J. Chem. Soc., Dalton Trans. (1975) 2410.
[35] C.L. Raston, A.H. White, J. Chem. Soc., Dalton Trans. (1975) 2422.
[36] Y. Mizobe, M. Hosomizu, Y. Kubota, M. Hidai, J. Organomet. Chem. 507 (1996) 179.
[37] A. Müller, W. Jagermann, Inorg. Chem. 18 (1979) 2631.
[38] B. Meyer, Chem. Rev. 76 (1976) 367.
[39] R. Steudel, Angew. Chem., Int. Ed. Engl. 14 (1975) 655.
[40] R.C. Elder, M. Trkula, Inorg. Chem. 16 (1977) 1048.
[41] R. Schneider, K. Wieghardt, B. Nuber, Inorg. Chem. 32 (1993) 4935.
[42] M.I. Bruce, C. Hameister, A.G. Swincer, R.C. Wallis, Inorg. Synth. 21 (1982) 78.
[43] M.A. Bennett, T.-N. Huang, T.W. Matheson, A.K. Smith, Inorg. Synth. 21 (1982) 74.
[44] SMART & SAINT Software Reference manuals, version 5.0, Bruker AXS Inc., Madison, WI, 1998.
[45] G.M. Sheldrick, SADABS Software for Empirical Absorption Correction, University of Göttingen, Germany, 2000.
[46] G.M. Sheldrick, SHELX-97. Program for Crystal Structure Solution, University of Göttingen, Germany, 1997.
[47] P.T. Beurskens, G. Admiraal, G. Beurskens, W.P. Bosman, S. García-Granda, J.M.M. Smits, C. Smykalla, The DIRDIF program system, Technical Report of the Crystallography Laboratory, University of Nijmegen, The Netherlands, 1994.
[48] G.M. Sheldrick, SHELXL-97. Program for the Refinement of Crystal Structures, University of Göttingen, Germany, 1997.
[49] teXsan, Structure Analysis Package, Molecular Structure Corporation, Woodlands, TX, 1992.